Biochimica et Biophysica Acta 1843 (2014) 1414–1426

Contents lists available at ScienceDirect

Biochimica et Biophysica Acta

journal homepage: www.elsevier.com/locate/bbamcr

# Oncofetal H19 RNA promotes tumor metastasis

Imad J. Matouk [a,*], Eli Raveh [a], Rasha Abu-lail [a], Shaul Mezan [a], Michal Gilon [a], Eitan Gershtain [a], Tatiana Birman [a], Jennifer Gallula [a], Tamar Schneider [a], Moshe Barkali [a], Carmelit Richler [a], Yakov Fellig [b], Vladimir Sorin [a], Ayala Hubert [c], Abraham Hochberg [a,1], Abraham Czerniak [d,1]

[a] Department of Biological Chemistry, Institute of Life Sciences, The Hebrew University of Jerusalem, Jerusalem 91904, Israel
[b] Department of Pathology, Hadassah Hebrew University Medical Center, Jerusalem 91240, Israel
[c] Department of Oncology, Hadassah University Hospital, Jerusalem 91000, Israel
[d] Department of HPB Surgery "A", Sheba Medical Center, Tel Hashomer, Tel Aviv 52621, Israel

ARTICLE INFO

*Article history:*
Received 6 November 2013
Received in revised form 15 February 2014
Accepted 26 March 2014
Available online 2 April 2014

*Keywords:*
Epithelial to mesenchymal transition
E-cadherin
Slug
Positive loop
H19
miR-675

ABSTRACT

The oncofetal H19 gene transcribes a long non-coding RNA(lncRNA) that is essential for tumor growth. Here we found that numerous established inducers of epithelial to mesenchymal transition(EMT) also induced H19/miR-675 expression. Both TGF-β and hypoxia concomitantly induced H19 and miR-675 with the induction of EMT markers. We identified the PI3K/AKT pathway mediating the inductions of Slug, H19 RNA and miR-675 in response to TGF-β treatment, while Slug induction depended on H19 RNA. In the EMT induced multidrug resistance model, H19 level was also induced. In a mouse breast cancer model, H19 expression was tightly correlated with metastatic potential. In patients, we detected high H19 expression in all common metastatic sites tested, regardless of tumor primary origin. H19 RNA suppressed the expression of E-cadherin protein. H19 up-regulated Slug expression concomitant with the suppression of E-cadherin protein through a mechanism that involved miR-675. Slug also up-regulated H19 expression and activated its promoter. Altogether, these results may support the existence of a positive feedback loop between Slug and H19/miR-675, that regulates E-cadherin expression. H19 RNA enhanced the invasive potential of cancer cells *in vitro* and enhanced tumor metastasis *in vivo*. Additionally, H19 knockdown attenuated the scattering and tumorigenic effects of HGF/SF. Our results present novel mechanistic insights into a critical role for H19 RNA in tumor progression and indicate a previously unknown link between H19/miR-675, Slug and E-cadherin in the regulation of cancer cell EMT programs.



## 1. Introduction

Delineating the molecular mechanisms underlying cancer recurrence and metastasis is vitally important. Tumor metastasis is the primary cause of mortality for most cancer patients, accounting approximately for 90% of all cancer deaths. One of the major mechanisms that mediates metastasis is EMT [1]. EMT is a prerequisite for invasion and dissemination of carcinoma cells [2]. Although EMT has been demonstrated in most cancer types, it has been particularly well studied in pancreatic cancer. EMT and dissemination have been shown to precede pancreatic tumor formation [3], and expression of EMT markers in pancreatic patient biopsies correlate with poor survival [4]. Pancreatic cancer EMT is triggered by hypoxia and inflammation and is involved in cancer cell stemness and multidrug resistance [5]. Consequently it is critical to find the molecular mediators of EMT, which would provide new targets for intervention in the process of metastatic recurrence of tumors.

H19 RNA is frequently over-expressed in the majority of human cancers, sometimes *via* loss of imprinting. Although its role in tumorigenesis is debated, the prevailing view is that H19 behaves like an oncogene [6,7]. Recent efforts to better characterize the H19 locus have revealed that it houses several overlapping transcriptions on the two DNA strands that can produce different transcriptional products [8]. In addition to H19 RNA itself, this locus also produces a micro-RNA called miR-675 [9], an antisense protein coding transcript called H19 opposite tumor suppressor (HOTS) [10], and a long intergenic antisense transcript called 91H [11]. Moreover, various splice variants have been reported [12]. The variety of products produced from the H19 gene locus may account for the discrepancies when dealing with H19 oncogenic effects. Moreover, H19 tumorigenic activity may depend on p53 status as we previously proposed [13].

In recent years, it has become increasingly clear that H19 RNA is essential for human tumor growth and that the H19 gene is regulated by a complex interplay of factors whose malfunctioning plays a critical role in tumorigenesis. In our recent studies we identified hypoxia as a key trigger enhancing the expression of the H19 gene, and we also characterized the major transcriptional interplay between its positive and

* Corresponding author. Tel.: +972 2 658 5456; fax: +972 2 548 6550.
*E-mail address:* imad.matouq@mail.huji.ac.il (I.J. Matouk).
[1] These authors contributed equally to the work.

http://dx.doi.org/10.1016/j.bbamcr.2014.03.023
0167-4889/

negative regulators. Furthermore, many of H19's downstream targets have been identified. A molecular mechanism integrating H19, p53 and hypoxia-inducible factor 1-α (HIF1-α) with the hypoxic stress response has been uncovered in which p53 suppression of H19 may, at least in part, involve interference with HIF1-α activity [6,13].

H19 is one of the transcriptional targets of c-Myc which strongly induces the expression of the maternal H19 allele and binds directly to un-methylated E-boxes close to the imprinting control region to potentiate tumorigenesis [14]. Given the strong association between H19 and c-Myc expressions, the essential role of H19 in transformation suggests that c-Myc-induced H19 expression contributes to tumor etiology and the strong oncogenic behavior of c-Myc.

Further supports for the involvement of H19 RNA in cell cycle progression have been provided by our group and others. We previously have shown that in serum starved conditions over-expression of the H19 gene can override cell cycle growth arrest and induce cells to enter the S phase, an effect which is accompanied by suppression of the expression level of the cyclin-dependent kinase inhibitor p57Kip2 [15]. This was supported by the findings of another group that H19 RNA is important for entry into the S-phase after recovery from serum starvation *via* E2F binding to its promoter [16]. H19 is suppressed by the tumor suppressor p53 [13,17]. Furthermore, miR-675, which is excised from exon one of H19, targets retinoblastoma tumor suppressor gene product [18]. All of these observations place the H19 locus at the core of cell cycle control, especially in the transition from G1 to S phase.

Numerous observations support the involvement of H19 RNA in the metastatic cascade, however, both functional and mechanistic data are lacking. The aim of the present study is to explore this issue. H19 expression was studied in biopsies selected to represent common metastatic sites and in a well established syngeneic mouse model of mammary cancer composed of a panel of cancer cell line variants each can perform definitive step in the metastatic cascade. We then studied H19's involvement in EMT utilizing well-established effectors and explored the molecular mechanism mediating H19 modulation using specific chemical inhibitor of signaling pathway and H19 over-expression approaches. These studies were followed by functional analyses using H19 over-expression and knockdown approaches. Our results presented here demonstrate that H19/miR-675 axis promotes tumor metastasis at least being part of the EMT process.

## 2. Materials and methods

### 2.1. Ethical statement

All procedures and the care given to the animals were approved by the local committee for animal welfare. Animals were kept in the Hebrew University's animal facility with water and food *ad libitum*. All experimental research on animals followed internationally recognized guidelines.

### 2.2. Cell culture conditions and treatments

All the cells used in this study were grown in Dulbecco's modified Eagle's medium (DMEM-F12) containing 10% fetal bovine serum. For hypoxic treatment, cells were grown in 1.2% $O_2$, 5% $CO_2$ for the indicated time before RNA and protein extractions.

For experiments involving TGF-β stimulation, Hep3B and UMUC3 cells were treated with 2 ng/ml TGF-β for 48 h and 24 h respectively before RNA extraction. When PI3K/AKT inhibitor (LY294002) was used, Hep3B cells were pre-treated with the inhibitor at a concentration of 20 μM for 1 h prior to TGF-β stimulation for 48 h. For experiment involving siRNAs, it is performed as previously described [6,13].

### 2.3. Reverse transcription for microRNA detection

Hsa-mir-675 and RNU48 miRNAs were reverse transcribed with the TaqMan miRNA reverse transcription kit (Applied Biosystems, Forster city, CA). 10 ng of total RNA and 3 μl of microRNA specific primers were used in 15 μL RT reaction buffer according to the manufacturer's instructions (Applied Biosystems).

### 2.4. Real-time quantitative PCR

H19, Snail and Slug expression levels were measured using real-time quantitative PCR (QPCR). The RNA levels were measured relative to beta actin (ACTB). PCR reactions were carried out in triplicates using FAM as the fluorescent detection dye and using the real-time PCR system Mx3000P (Stratagene, La Jolla, CA). The H19, Snail and Slug TaqMan reactions were optimized and shown to have an equal amplification efficiency as the beta actin. 2 μl of each cDNA was amplified in 20 μl volume PCR reaction containing the human H19 forward primer TGCTGCACTTTACAACCACTG; H19 reverse primer ATGGTGTCTTTGATGTTGGGC; and the TaqMan probe TCGGCTCTGGAAGGTGAAGCTAGAGGA which spans the junction of exons 4 and 5, thus providing specificity to the RNA and not the genomic DNA [45]. For mouse H19, PCR reaction contained the forward primer CGGCGACGGAGCAGTGAT; reverse primer ACCTGTCATCCTCGCCTTCA; and the TaqMan probe TGGAGACTAGGCCAGGTCTCCAGCA. Primers and TaqMan probes for Snail and Slug were as follows: Snail: ACCACTATGCCGCGCTCTT; and GGTCGTAGGGCTGCTGGAA; Slug: TGTTGCAGTGAGGGCAAGAA; and GACCCTGGTTGCTTCAAGGA′; the TaqMan probe for Snail: TCGTCAGGAAGCCCTCCGACCC; and Slug: AGGCTTCTCCCCCGTGTGAGTTCTAATG. Each primer was placed in a different exon to avoid amplification of contaminating genomic DNA [46]. For human ACTB the forward primer was GACAGGATGCAGAAGGAGATCACTG; the reverse primer CGCCGATCCACACGGAGTACTT; and TaqMan probe ATGAAGATC AAGATCATTGCTCCTCCT. Whereas for mouse (Actb), the forward primer was GACAGGATGCAGAAGGAGATTACTG; reverse primer CCACCGATCCACACAGAGTACTT; and TaqMan probe CCATGAAGATCAAGATCATTGCTCCTCCT. All the DNA sequences listed above are written in 5' to 3' direction. 1× ABsolute Blue QPCR low ROX mix (ABgene) was used with the following cycling parameters: 95 °C for 15 min, followed by 40 cycles of 95 °C for 15 s and 60 °C for 1 min. All QPCR runs included a 6-points standard curve of known dilution; the efficiency of PCR was calculated from the slope of the standard curve and was within the range of 90–110%.

For miRNA, hsa-mir-675 was quantified utilizing TaqMan specific microRNA assay kit (Applied Bioystems). The expression of small nucleolar RNA RNU48 served as an endogenous control for normalization. 1.33 μl of the 1:15 dilution from the RT reaction and TaqMan Universal PCR Master Mix, No AmpErase UNG (Applied Biosystems) were used in 20 μl QPCR reaction mix. The reaction was initiated at 95 °C for 10 min, followed by 40 cycles of 95 °C for 15 s, and 60 °C for 1 min.

### 2.5. Patient biopsies and LNA in situ hybridization

*In situ* hybridization (ISH) for H19 was done with specific 5′ end digoxigenin (DIG) labeled locked nucleic acid based probe (LNA), (Exiqon Inc, MA). The LNA-modified probes are used to enhance the detection, achieve superior sensitivity and improve specificity of the ISH reaction. Paraffin sections cut from archival material (paraffin blocks) selected to represent metastasis to common sites were subjected to ISH for H19. Approximately 5 μm thick sections from tissue blocks were deparaffinized in xylene and rehydrated in descending grades of alcohol, followed by treatment with 0.1% Triton-100/PBS. The slides were then washed with PBS (pH 7.5) and permeabilized by being incubated in 10 μg/ml proteinase K (Ambion) for 25 min at 37 °C. Slides were rinsed in PBS, and then refixed for 5 min in 4% paraformaldehyde/PBS. Thereafter, they were rinsed in

PBS and acetylated for 10 min in fresh acetic anhydride diluted 1/400 in 0.1 M triethanolamine (Sigma) at pH 8.0, rinsed in PBS, then RNase-free water, dehydrated, and air dried.

The hybridization buffer contained 50% deionized formamide, 0.3 M NaCl, 20 mM Tris–HCl (pH 7.4), 5 mM EDTA, 10 mM $NaH_2PO_4$ (pH 8.0), 10% dextran sulphate, 1× Denhardt's solution, and 0.5 μg/ml yeast tRNA. Each slide was covered with 30 μl of the hybridization solution containing DIG labeled LNA probes. The negative controls either omitted the probe or used scrambled probe. Human beta-actin DIG labelled LNA probe was used as a positive control.

Slides were covered with siliconized coverslips and hybridization was performed at 52–54 °C for at least 14 h in a humidity chamber. After hybridization, coverslips were gently floated off in 2× SSPE + 0.1% SDS solution for 5 min. Slides were washed with 0.1× SSPE + 0.1% SDS for 10 min at 55 °C followed by rinsing twice in 2× SSPE, equilibrated in buffer 1 (100 mM Tris–HCl and 150 mM NaCl, pH 7.5). This was followed by blocking with 2% sheep serum for 30 min (to avoid non-specific crossreactions of the primary antibody), after that slides were incubated with 1:2,000 anti-DIG-AP Fab fragments antibody (Roche Applied Sciences, Indianapolis, IN) in a humidified chamber for 3 h at room temperature, followed by two washes in buffer 1. Slides were equilibrated in buffer 2 (100 mM Tris–HCl, 100 mM NaCl, and 50 mM MgCl2, pH 9.5) for 10 min. The color reaction was carried out by incubation in 5-bromo-4-chloro-3-indolyl phosphate (BCIP)/nitro blue tetrazolium (NBT) color solution (Roche Applied Sciences, Indianapolis, IN) with 1 mM levamisole for 12–16 h in a humidity chamber and allowed to develop in the dark at room temperature. The reaction was stopped in buffer 3 (10 mM Tris–HCl and 1 mM EDTA, pH 7.4) for a few minutes. Finally, the sections were counterstained with 3% Giemsa stain and quickly dehydrated. The slides were then mounted and observed under Olympus B×40 microscope.

### 2.6. Western blot analyses

Cell protein was extracted by TRI reagent solution (Sigma) and loaded to 4–12% polyacrylamide precast gels. Gels were blotted on PVDF sheets and their residual content was analyzed for visually estimated quantification by Coomassie staining. The blots were subjected to the following antibodies: goat anti N-Cadherin 1:1000 (Santa Cruz); mouse anti E-Cadherin, 1:1000 (Abcam); mouse anti GAPDH 1:2500 (Santa Cruz). Secondary horseradish-peroxidase antibodies (anti-mouse $10^{-4}$, otherwise: 1/30,000) were from Jackson. SuperSignal West Pico Chemiluminescent Substrate (Pierce) was used as a substrate.

### 2.7. In vitro invasion assay

To assess the effect of H19 RNA on the metastatic potential of cells *in vitro*, we used the non-metastatic hepatocellular carcinoma Hep3B cell line and BD biocoat matrigel invasion chambers (BD Biosciences) according to the manufacturer instructions. Briefly 50,000 Hep3B cells and its H19 over-expression variant were plated seperately in serum free medium in invasion chambers which contained an 8 micron pore size PET membrane with a thin layer of matrigel basement membrane matrix. As a chemo-attractant, the same medium with 10% fetal calf serum was placed in the wells which contained the invasion chambers, and the cells were incubated for 18 h. For measurement of cell invasion, non-invading cells were removed from the upper surface of the membrane by firm scrubbing using cotton swabs. Cells were then fixed by methanol treatment, and stained with Giemza. Excess stain was washed away using DDW and invading cells were quantified using Image Pro-Plus. Each type of cell was plated in triplicate, and the experiment was performed twice.

### 2.8. Generation of cell lines ectopically expressing H19 RNA

H358, Hep3B and Panc-1 cells were transfected with an expression vector in which the H19 gene was under the constitutive transcriptional control of the CMV promoter, producing cells with stable over-expression of H19 RNA. Cells were transfected with the same vector backbone with an empty transcriptional unit as control.

24 h before transfection, cells were plated into 6 well plates at a density of $1 \times 10^5$ cells/per well in antibiotic free medium. Transfections were carried out using lipofectamine 2000 and 2 μg plasmid per well as previously described [13]. 48 h after transfection, cells were diluted and divided into new culture dishes. Cells were selected after being grown 15 days in a medium containing 500 μg/ml G418 sulfate antibiotic (Gibco-BRL).

### 2.9. Anchorage-independent growth assay

Lung cancer cell lines A549 and H358 were each seeded in 60 mm plates, and transfected in duplicates with siRNA duplexes targeting H19 RNA, with an unrelated control siRNA targeting the luciferase (siLUC), or left to grow with no treatment (NT). 12 h post transfection, one plate of each duplicate were exposed to hypoxic conditions while the others remained in normoxia for another 24 h. Cells were washed with PBS, trypsinized and counted. $5 \times 10^3$ cells from each 60 mm plate were then seeded in 6-well plates containing 0.35% top and 0.8% base high DNA grade agarose, in two sets of triplicates. In one set, cells were left to grow in normal growth conditions with 1 ml medium renewed every 3–4 days. In the other set, growth medium was supplemented with HGF at final concentration of 20ng/ml for A549 and 40 ng/ml, for H358. 4 weeks (A549 cells) and 6 weeks (H358 cells) post seeding, colonies were dyed with 0.05% crystal violet and counted under the light microscope. Colony size and shape were also noted. Colony counting procedure: a transparent paper was cut to be at the same shape and size as one of the wells. It was divided into 59 small (0.4 × 0.4 cm) squares. Colonies in 8 random squares were counted (for this count standard deviation did not exceed a maximum value of ±3 for wells that were not treated with HGF and ±5 for those that were). The mean value of this count was then multiplied by 59 to give the final absolute number of colonies per well. The standard errors presented are for the mean of three triplicates.

### 2.10. In vivo experiments

To check the effect of H19 RNA on metastatic potential of cells *in vivo*, we used the human lung carcinoma H358 cell line. We generated an H19 over-expressing variant with its control being cells transfected with an empty plasmid as described above. Confluent cells were trypsinized to a single cell suspension and resuspended in PBS. $1 \times 10^6$ cells (in 150 μl volume) were intravenously injected into the tail vein of 6–8 weeks\ old female CD1 nude mice. 28 days post injections, mice were sacrificed and their lungs, brains and livers were examined for both macro and micro metastasis.

### 2.11. Semi-quantitative RT-PCR analyses

Reverse transcription was performed as previously described [13]. Details of the PCR conditions and the PCR primer sequences are available upon request.

### 2.12. Plasmid design

The full length H19 gene driven by the CMV promoter was designed by GeneArt and fully sequenced. The H19 cDNA was cloned into pCMV-Skript. The control vector was designed without the H19 insert. The Slug expression plasmid (19293) was from Addgene [30]. For the generation of the expression vector CMV-Slug, Slug insert present in the vector 19293 was digested with BamH1, EcoR1 restriction enzymes and cloned into the backbone pCMV-Skript vector. The control vector was designed without the Slug insert.

### 2.13. Statistical analyses

All data are expressed as mean ± standard deviation. The differences between groups were analyzed using student's *t* test. The differences were deemed statistically significant at $p < 0.05$.

## 3. Results

### 3.1. Classical inducers of EMT modulate H19 gene expression

Several factors have been shown to induce the EMT process. The most established and relatively well studied effectors are the transforming growth factor beta (TGF-β), hypoxia, hepatocyte growth factor/scatter factor (HGF/SF), and multi-drug resistance. Remarkably, we found that all of these inducers have a common dominator; the ability to induce H19 gene expression.

#### 3.1.1. TGF-β induces H19 expression and miR-675 level through the PI3K–AKT pathway

To test the effect of TGF-β on H19 expression, we treated human hepatocellular carcinoma Hep3B cells with 2 ng/ml TGF-β for 48 h. As shown in Fig. 1A (first panel) and B, TGF-β treatment resulted in a significant induction of H19 RNA. To confirm that TGF-β treatment of Hep3B cells induces EMT, we checked for modulation of established EMT markers. Transcription factors of the Snail family, including Snail and Slug, are key inducers of EMT [19]. These two transcription repressors are the most widely studied effectors of EMT and are situated at the core of several signaling pathways. As shown in Fig. 1A (second panel) & 1C, TGF-β treatment resulted in an up-regulation of the expression levels of both EMT markers. H19 gene function could be mediated by miR-675 processed from H19 exon 1. To check if TGF-β also affects miR-675 levels, we quantified miR-675 before and after TGF-β treatment. As shown in (Fig. 1D), TGF-β significantly induced miR-675 level along with H19 induction ($p < 0.01$).

We sought to identify the signaling pathway mediating the up-regulation of both H19 and miR-675 in response to TGF-β treatment. As TGF-β is well known as a promoter of EMT, the phosphatidylinositide 3-kinase PI3K/AKT axis is emerging as a central feature of EMT. Enhanced TGF-β receptor signaling was reported to maintain hyperactive PI3K/AKT signaling, which in turn promoted EMT [20].

The effect of LY294002, a highly selective inhibitor of PI3K [21] on EMT triggered by TGF-β treatment was investigated. Suppression of the PI3K/AKT pathway before TGF-β treatment resulted in a significant decrease in the level of the EMT marker Slug to below that of non-stimulated cells (Fig. 1C; $p < 0.01$). This indicates that TGF-β induction of Slug in Hep3B cells is dependent on the PI3K/AKT pathway. To test if TGF-β induction of H19 expression and miR-675 levels involves the PI3K/AKT pathway, we investigated their modulation. While H19 was induced by TGF-β treatment in Hep3B cells, this induction was abolished through pre-treatment of the cells with LY294002 prior to TGF-β manipulation (Fig. 1B; $p < 0.01$) and miR-675 was also not induced (Fig. 1D; $p < 0.01$). These results mechanistically link the induction of both H19 RNA and miR-675 in response to the TGF-β induced EMT program to the PI3K/AKT pathway.

We further explored the effect of TGF-β on H19 expression using a well-characterized mice cell line model of mammary carcinogenesis that depends on the collaboration of the Ha-Ras oncoprotein and TGF-β. Ha-Ras-transformed EpH4 mammary epithelial cells give rise to

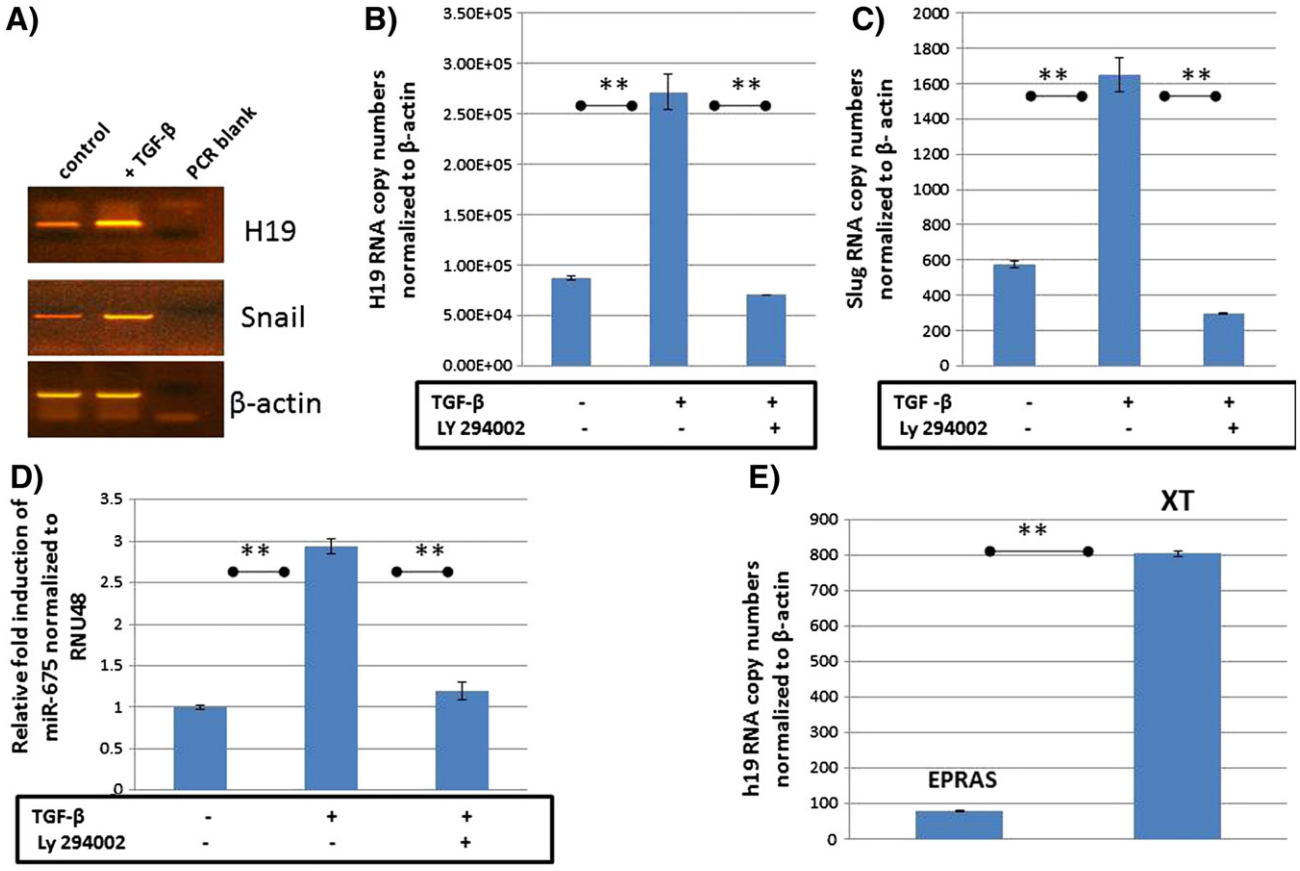


**Fig. 1.** TGF-β induction of Slug, H19 and miR-675 expressions was dependent on the PI3K/AKT pathway. (A) TGF-β induced H19 and Snail expressions in Hep3B cells as analyzed by semi-quantitative RT-PCR analyses. The integrity of the RT-PCR analyses was verified by analyzing β-actin expression. (B &C &D) The up-regulation of H19, Slug and miR-675 expressions by TGF-β treatment was dependent on the PI3K/–AKT pathway as determined by QPCR analyses. (E) In a mouse model of mammary carcinogenesis, EMT induced by TGF-β was associated with an approximate 10 fold difference in h19 RNA level being higher in mesenchymal cells (×T) relative to epithelial cells (EPRAS) as determined by QPCR analyses. **P < 0.01.

oncogenic fully-polarized cells, EpRas [22]. These cells can undergo EMT in response to TGF-β both *in vitro* and *in vivo* giving rise to the mesenchyme-like EpRas × T cells. We investigated whether H19 is differentially expressed in EpRas and EpRas × T cells. As shown by QPCR analysis, the H19 level was significantly higher in mesenchyme-like EpRas × T cells than in the epithelial EpRas cells (Fig. 1E; $p < 0.01$).

*3.1.2. EMT induced by hypoxia is associated with a strong induction of both H19 RNA and miR-675*

We sought to determine whether hypoxia induced EMT is also accompanied by the modulation of H19 gene expression and miR-675 levels. We used the MDA-MB- 468 breast cancer cell line that undergoes EMT when cultured in hypoxic conditions [23]. MDA-MB- 468 cells cultured in hypoxic conditions demonstrated an approximately 100-fold increase in H19 mRNA compared with cells that were maintained in normoxic conditions as quantified by QPCR analyses (Fig. 2A; $p < 0.01$). To test if EMT markers are also influenced by hypoxia, we analyzed Snail and Slug expression levels. As shown in Fig. 2B & C, hypoxic treatment significantly induced both of these EMT markers ($p < 0.05$). Hypoxia also increased miR-675 levels along with the H19 induction (Fig. 2D;$p < 0.01$). These results demonstrate that hypoxia induced EMT was associated with profound inductions of H19 RNA expression and increased miR-675 levels.

*3.1.3. Acquisition of chemo-resistance and EMT phenotype is associated with an induction of H19 RNA in ovarian carcinoma cells*

Increasing evidences suggest that EMT is important for the acquisition of a drug resistant phenotype in various types of human cancers [24]. EMT gene signatures correlate with the presence of drug resistance [25]. The well characterized cisplatinum resistant ovarian adenocarcinoma model (A2780cis), which has both the morphological and the phenotypic hallmarks of EMT [26] represents a good model to test for differential expression of H19 RNA compared to its epithelial parental line (A2780). We examined the morphological characteristics of these cell lines during exponential growth. In accordance with previous work (Haslehurst et al. 2012), we demonstrated features of a mesenchymal phenotype in the resistant cells (Fig. 3A & B). H19 RNA was induced approximately 20-fold in the chemo-resistant cell line with the mesenchymal phenotype (Fig. 3C; $p < 0.01$). This correlated with an increase in the expression level of the EMT transcription factor Slug which was also induced 12-fold in the chemo-resistant mesenchymal cells (Fig. 3D; $p < 0.01$).

*3.2. H19 gene is highly expressed in common metastatic sites regardless of tumor primary origin and its expression level significantly correlates with the metastatic potential of breast cancer cells*

We compared the expression levels of the H19 gene in common metastatic sites in selected biopsies of different tumor primary origin. A set of slides from biopsies of five patients (Fig. 4.1–4.5) with metastases to lung ($n = 2$), brain ($n = 1$), liver ($n = 1$) and bone ($n = 1$), together with the primary tumors when available for the same patient, were subjected to *in situ* hybridization (ISH). High H19 RNA expression was detected in all metastatic sites tested, sometimes with higher expression levels relative to the tumor primary sites. In the case of serious endometrial carcinoma and its lung metastasis (Fig. 4.2A & B) H19 expression was higher in the metastatic sites. H19 expression was similar in peripheral cholagiocarcinoma and its lung metastasis (Fig. 4.1A & B) and that of duct carcinoma of the breast and its brain metastasis (Fig. 4.3A & B). H19 RNA was strongly expressed in liver metastasis of colon carcinoma (Fig. 4.4) consistent with a previous report [27]. We also observed strong H19 RNA expression in bone metastasis of breast

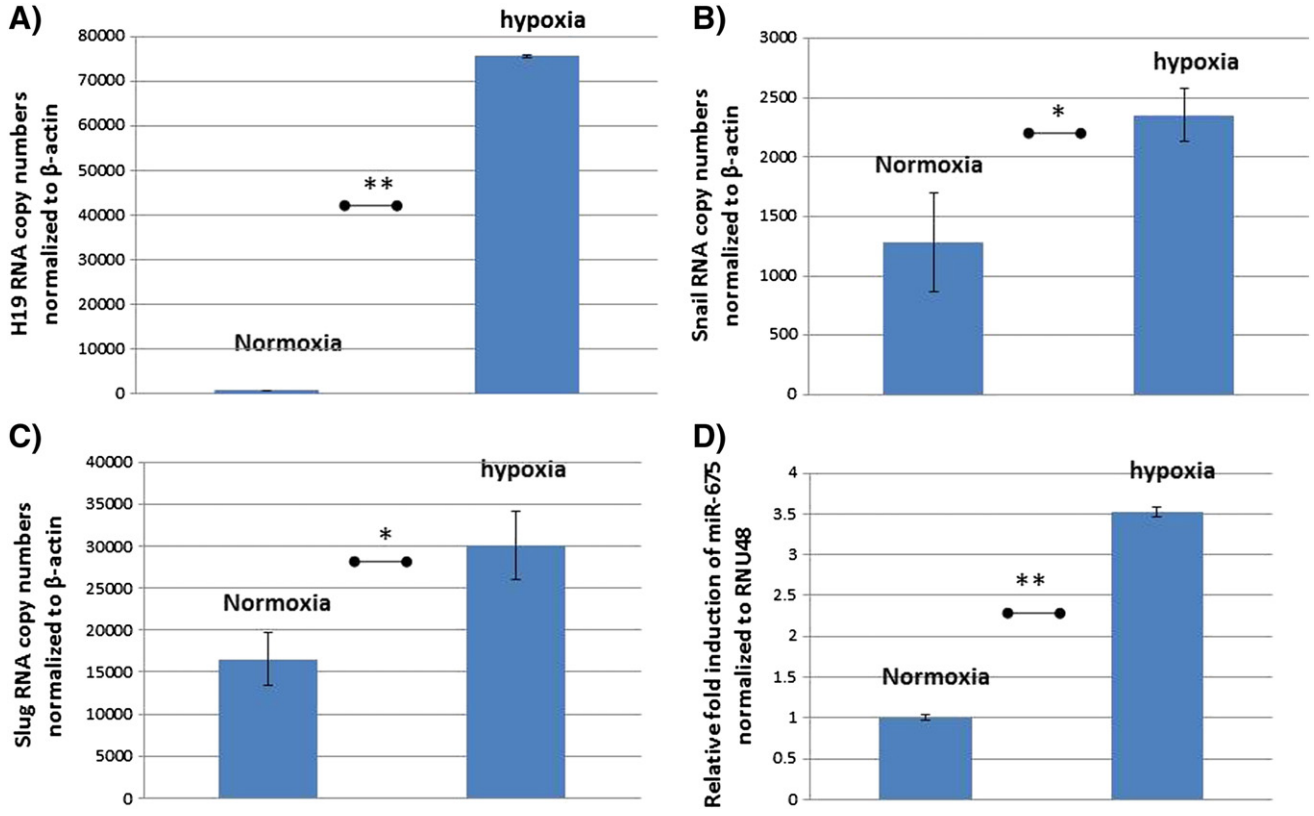


**Fig. 2.** Human breast carcinoma cells triggered to undergo EMT by hypoxia manifested a profound up-regulation of both H19 RNA and miR-675 along with EMT markers. The human breast carcinoma cells (MDA-MB-468) were cultured in normoxic conditions or in 1.2% $O_2$ hypoxic conditions for 48 h before RNA extraction. Shown are (A) QPCR analyses for H19 RNA with an approximate 100 fold induction by hypoxia. (B & C) Snail and Slug EMT markers showed higher expression level in hypoxia. (D) miR-675 was also induced by hypoxic EMT. **$P < 0.01$, *$P < 0.05$.

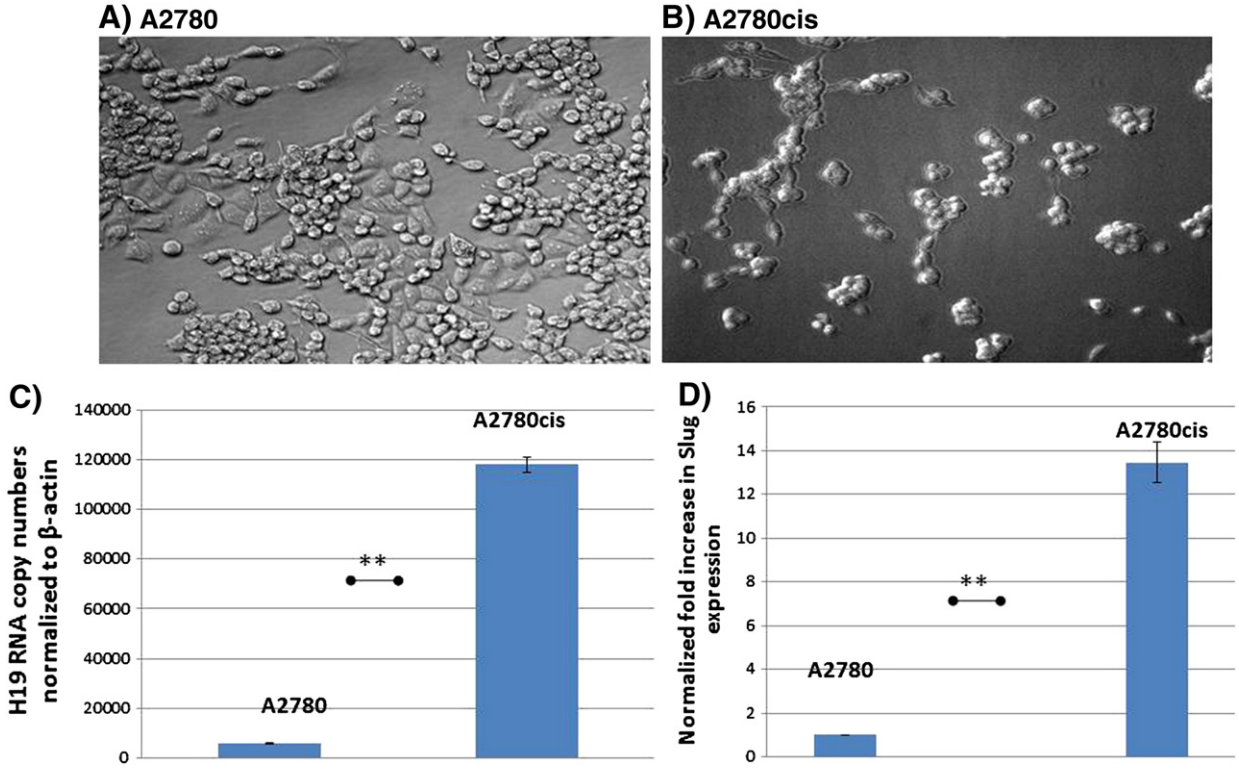


**Fig. 3.** The cisplatinum resistant ovarian cancer cells (A2780cis) exhibited mesenchymal phenotypes associated with an increase in the expression levels of both H19 and Slug. (A & B) The parental A2780 ovarian carcinoma cells, and its cisplatinum resistant variant visualized under 20× magnification showed different morphology. The drug resistant variant (B) have morphological features of mesenchymal cells with more fibroblastic appearance and demonstrate reduced intercellular contacts. These cells showed significantly higher levels of both H19 (C) and Slug (D) expressions as tested by QPCR analyses. **P < 0.01.

carcinoma (Fig. 4.5). Overall, H19 RNA was highly expressed in all common metastatic sites examined regardless of the tumor primary origin.

Several syngeneic tumor lines with a spectrum of metastatic phenotypes have been isolated from a spontaneous mammary tumor in a BALB/cfC3H mouse [28]. The tumor lines were categorized as non-metastatic (67NR), weakly metastatic to lymph node (168FARN) or lung (66 cl4), or highly metastatic to lymph node, lung, and bone (4 T1). This model has been extensively used to search for key regulators of the metastasis cascade [29]. We sought to determine if the h19 gene is differentially expressed in these sub-lines with different metastatic potential. RT-QPCR analyses revealed that h19 is highly expressed in the 4 T1 cell line in comparison to the other lines which had no to moderate h19 expression. Notably, an approximate 250-fold difference in the expression level of h19 was noted between the non-metastatic 67NR cells and the highly metastatic 4 T1 cells (Fig. 5; $p < 0.01$). Furthermore the expression level of h19 was significantly higher in the 168FARN cell line (weakly metastatic to lymph node; $p < 0.01$) and in the 66 cl4 cell line (weakly metastatic to lung; $p < 0.01$).

### *3.3. Evidence supporting the existence of a Slug-H19 positive loop mediated through miR-675 involved in the suppression of the epithelial marker E-cadherin*

We hypothesized that transcription factors that regulate EMT can modulate H19 RNA expression. Slug is a mediator of EMT and tumor metastasis. We utilized the ovarian carcinoma A2780 parental line as a model and transiently transfected it with a plasmid vector that drives the expression of Slug under the control of the (CMV) promoter after sub cloning it into the backbone pCMV-Skript vector [30 and material and methods]. As shown in Fig. 6A, Slug significantly up-regulated the expression level of H19 RNA ($p < 0.01$).

Since it is a transcription factor, we hypothesized that Slug may up-regulate H19 expression by enhancing its transcription. To check this possibility, we cloned an approximately 0.8 Kbp H19 promoter upstream of a luciferase reporter. We then co-transfected the H19 promoter with the Slug expressing plasmid, or the H19 promoter with an empty inert vector into the A2780 ovarian carcinoma cell line. As shown in Fig. 6B, Slug significantly up-regulated H19 promoter activity about 3-fold ($p < 0.01$). To check if this effect was a general one, we co-transfected Slug expressing vector with the Luc-4 vector which drives the expression of luciferase under the control of the SV40 promoter. Co-transfection with Slug did not modulate the activity of the SV40 promoter as shown in Fig. 6B. Bioinformatic analysis revealed that the 0.8 Kbp promoter of H19 does not contain a Slug binding site (data not shown), suggesting that this effect may be indirect.

In order to determine if H19 could modulate Slug expression, we chose the pancreatic cancer cell line Panc-1, since it has a low Slug expression (Fig. 6C) and we were searching for inducers. Ectopic expression of H19 RNA using the vector that drives the expression of H19 gene under the control of the CMV promoter, although resulted in mild up-regulation of H19 RNA (1.8-fold; data not shown), highly induced Slug expression (Fig. 6C), but did not induce Snail expression (Fig. 6D). The enhancement was abrogated when an H19 expression plasmid mutated in the seed region of miR-675 was used (Fig. 6C). Interestingly, this was accompanied by suppression of the Slug target E-cadherin in H19 over-expressing Panc-1 cells, but not in cells transfected with the mutated miR-675 version of the plasmid (Fig. 6F), indicating that this finding may have functional consequences. Altogether, these results indicate that H19 up-regulated Slug expression and that this was dependent on intact miR-675 and resulted in the suppression of the epithelial marker E-cadherin.

We then explored if TGF-β induced Slug up-regulation in Hep3B cells is dependent on H19 RNA. We stably transfected Hep3B cells with a plasmid expressing H19 shRNA, or a control shRNA. H19 shRNA transfection resulted in very efficient H19 knockdown (data not shown). These cells were then stimulated to undergo EMT by TGF-β

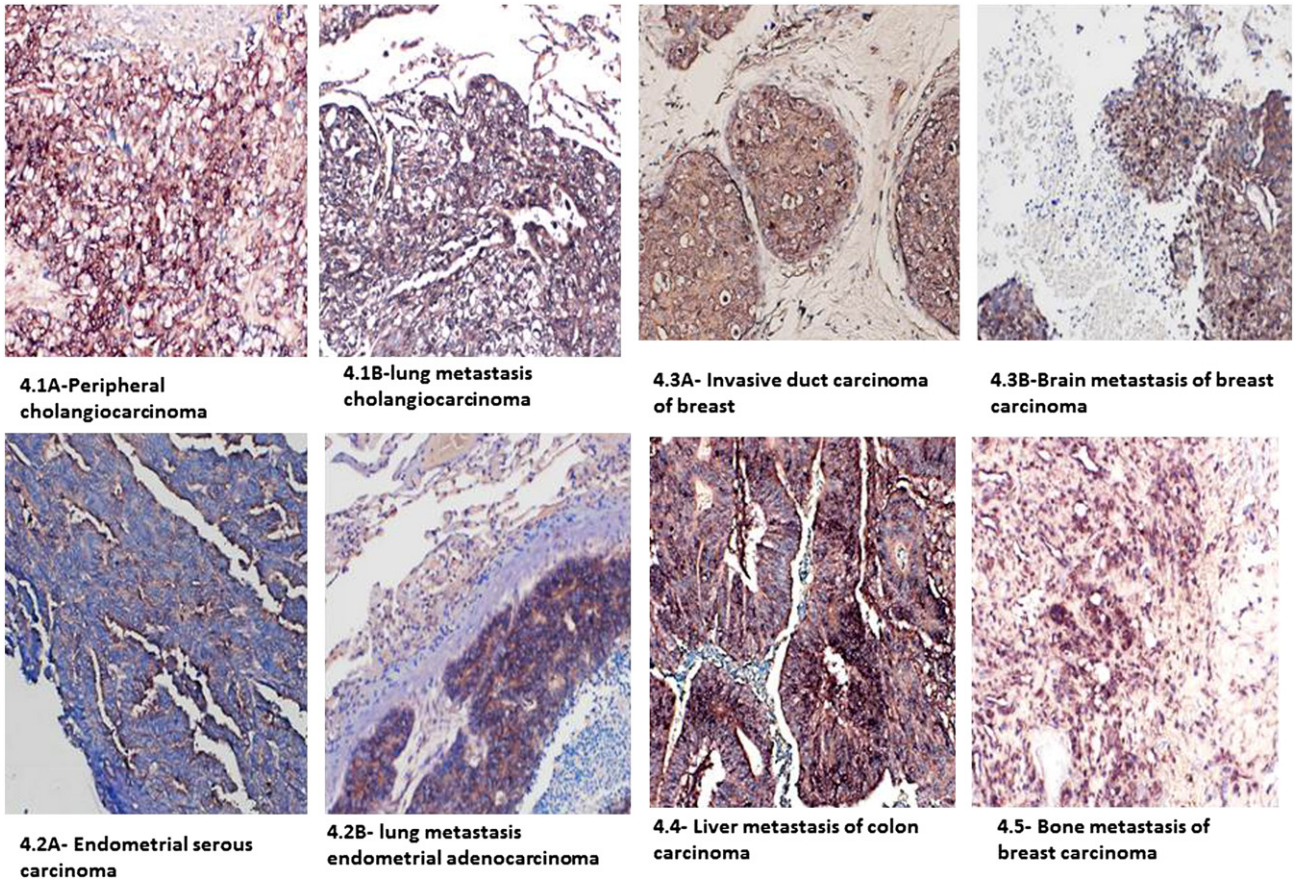


**Fig. 4.** High H19 expression level presented in all common metastatic sites tested regardless of tumor primary origin. ISH results showed that H19 was expressed in all selected biopsies derived from 5 patients (4.1–4.5) as representative samples for the most common metastatic sites. Primary tumors were also available for 3 patients (4.1A, 4.2A and 4.3A). The specifications of each tumor type described under each part of the figure.

as indicated in the materials and methods. Our results show that Slug is induced by TGF-β as previously described but this is dependent on H19 RNA (Fig. 7A).

We next showed using two H19 siRNAs targeting different regions of H19 RNA that H19 enhanced the induction of Slug in response to TGF-β treatment in bladder cancer UMUC3 cells. This

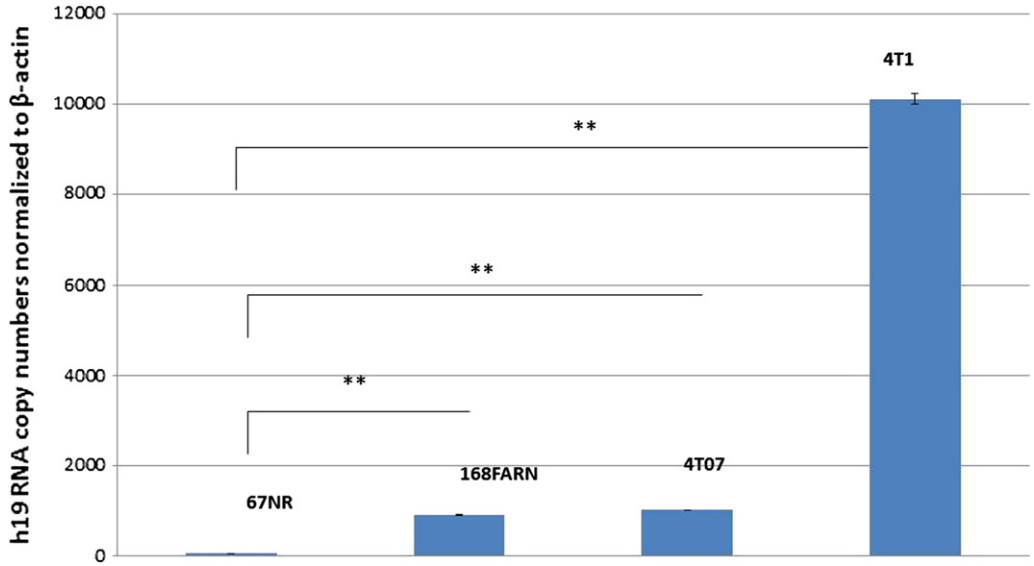


**Fig. 5.** Highest h19 expression level was detected in cells with the highest metastatic potential. An approximate 250-fold difference in h19 expression level between the non-metastatic 67NR cells and the highly metastatic 4T1 cells was detected by QPCR analyses. This widely recognized mice cell line variants isolated from a spontaneous mammary tumors known to have a spectrum of metastatic phenotype as described in the results section. **P < 0.01.

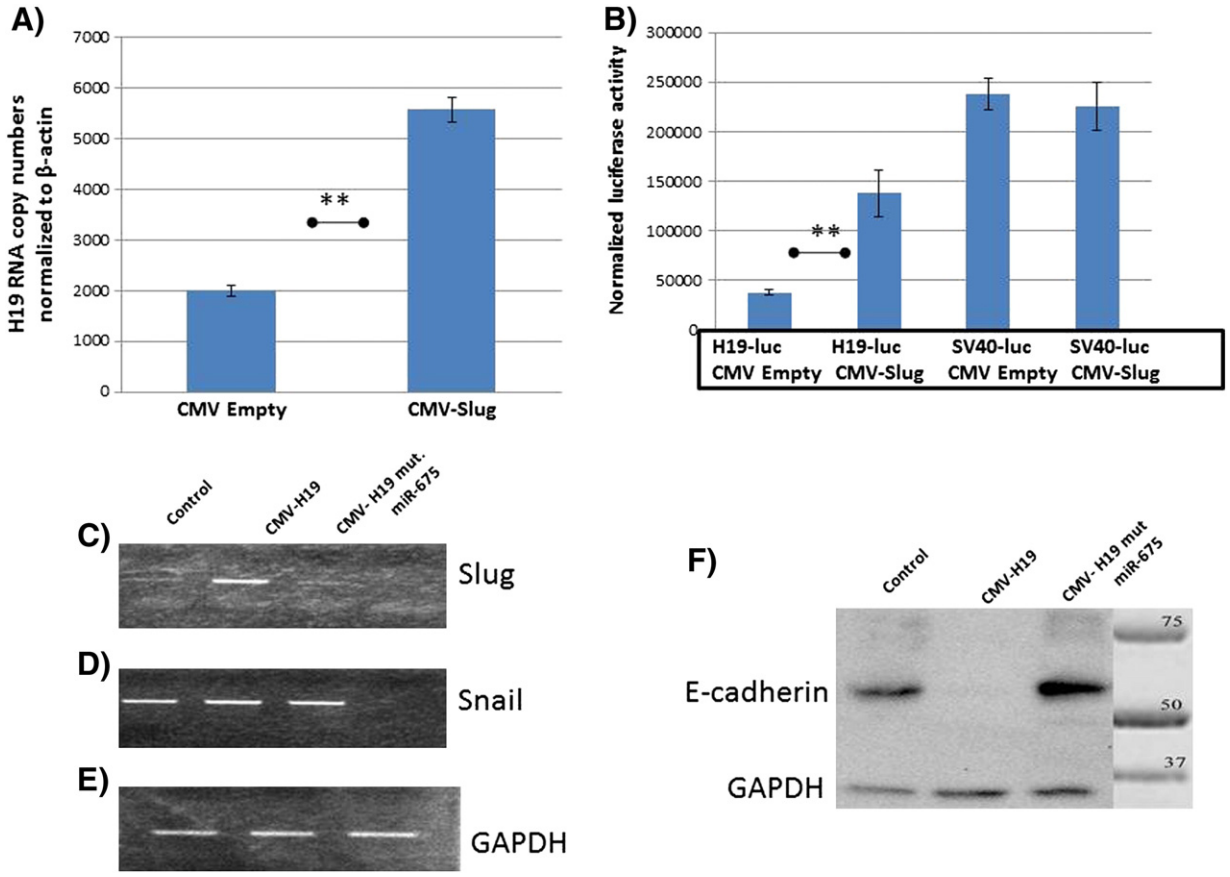


**Fig. 6.** Evidence of a Slug-H19-miR675 positive feedback loop controlling E-cadherin expression. (A) The ovarian carcinoma cell line (A2780) was transfected with Slug expression vector driven by CMV promoter (CMV-Slug) or a control vector (CMV-Empty). Results showed an up-regulation of the expression level of H19 RNA by Slug as detected by QPCR analyses (B). Slug enhanced H19 but not SV40 promoter activity as measured by co-transfection of Slug expression vector with either H19 or SV40 promoters that drived the expression of luciferase reporter. (C) H19 induced Slug expression in Panc-1 cells was dependent on intact miR-675. Stable Panc-1 clones either over-expressing H19 RNA, H19 RNA with miR-675 mutated in seed region , and a control vector (CMV promoter with empty insert) were generated and Slug expression level was checked by RT-PCR analyses (D) RT-PCR analyses for Snail showing no modulation. (E) RT-PCR analyses for GAPDH to test for RT-PCR integrity. (F) Western blot analyses of E-cadherin protein showing that the consequent up-regulation of Slug by H19 with an intact miR-675 may be reflected by the complete abolishment of E-cadherin protein level. **$P < 0.01$.

step was taken to rule out the possibility of siRNA off-target effect. Treatment of UMUC3 cells with TGF-β significantly induced Slug expression of about seven fold ($p < 0.01$). Both H19 siRNAs resulted in very efficient H19 knockdown (data not shown). Knockdown of H19 RNA prior to TGF-β treatment significantly attenuated Slug induction (Fig. 7B; $p < 0.05$).

We then investigated the involvement of H19 RNA in the suppression of E-cadherin in two other cancer cell lines of different origin—Hep3B cells (hepatocellular carcinoma) and H358 cells (lung carcinoma). Clones of these cells ectopically over expressing H19 under the control of the CMV promoter were generated. We verified very high H19 up-regulation by RT-PCR analyses (data not shown). Western blot analyses revealed that H19 over-expression resulted in no detectable level of E-cadherin protein in both cell lines (Fig. 7D) and an up-regulation of N-cadherin in H358 cells (Fig. 7C).

### *3.4. H19 enhances migratory potential of cells in vitro and enhances tumor metastasis in vivo*

In light of our findings, we decided to functionally assess the effect of H19 RNA over-expression on the invasive ability of cancer cells *in vitro* and the metastasizing ability *in vivo*. Forced expression of H19 gene in the non-invasive Hep3B cells enhanced *in vitro* cell invasion of about two fold as quantified by Image Pro-Plus (data not shown) compared with the control cells which contained an empty vector. This can be seen as an increase in the intensity of the blue color of the Giemza stain (Fig. 8A & B), which stains cells that successfully invade an artificial membrane. Shown are representative samples.

*In vivo* metastasis assays were performed to ascertain whether H19 RNA has a role in the metastatic behavior of lung cancer cells. Forced expression of H19 RNA in H358 cells enhanced their capacity to generate lung metastases after being injected intravenously into the tails of athymic mice. H358 control cells (stably transfected by an empty vector) and H358-CMV-H19 cells (ectopically expressing H19 under the transcriptional control of CMV promoter) were injected into the tail vein. 28 days post-injection, 33% of the mice injected with H358-CMV-H19 cells ($n = 6$) had visible metastasis in their lungs while none of the mice injected with the H358 control cells ($n = 6$) had visible metastasis in any organ.

Histological analyses of the lungs of the injected mice showed that the majority (5/6) of the mice injected with H358-CMV-H19 had developed several micro-metastatic foci in many locations in the lung compared to 3/6 mice that had developed fewer micro-metastasis foci of smaller size in the H358 control cell group. Representative histology for both groups of mice is shown in Fig. 8C & D.

Altogether, our *in vitro* and *in vivo* functional analyses suggest that H19 RNA expression in hepatocelluar and lung carcinomas plays an important role in enhancing the invasive potential of the cells for the former and in the acquisition of high metastatic potential of the cells for the later.

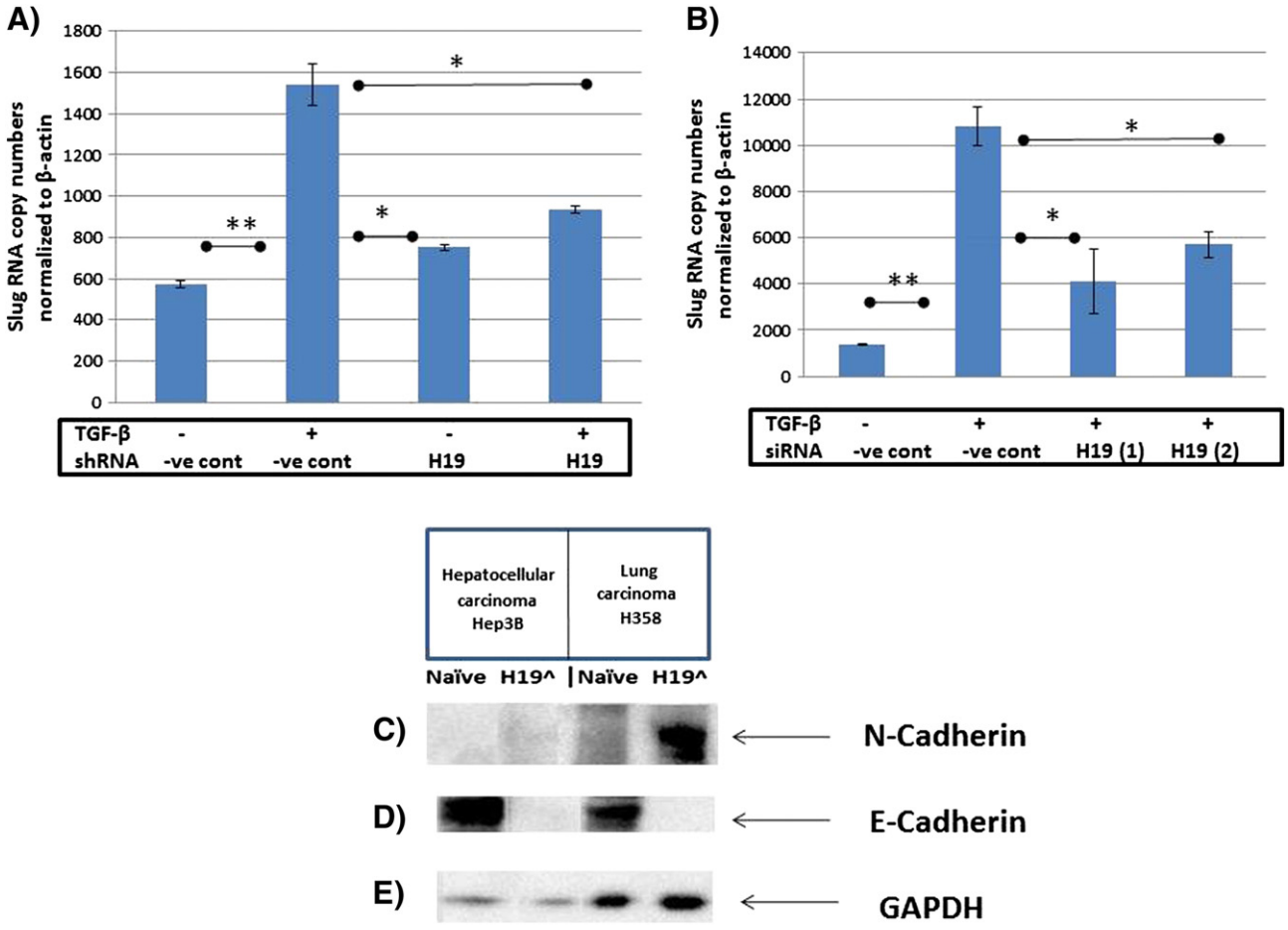


**Fig. 7.** Knock-down of H19 attenuated Slug induction in response to TGF-β, whereas H19 RNA over expression abolished the epithelial marker E-cadherin protein level. Stable clones of Hep3B cells either transfected with H19 shRNA or negative control shRNA were generated. TGF-β treatment resulted in the induction of Slug expression that depended on H19 RNA. Shown (A) RT-QPCR analyses for Slug.(B) To verify that Slug attenuation is not attributed to H19 shRNA off-target effect, and to broaden this observation, we transiently knocked down H19 RNA in bladder carcinoma UMUC3 cell line by two different H19 siRNAs prior to TGF-β stimulation. Again Slug induction by TGF-β depended on H19 RNA as quantified by QPCR analyses. **P < 0.01, *P,0.05. In addition stable clones of hepatocellular carcinoma (Hep3B) cells and lung carcinoma (H358) cells over-expressing H19 were generated and subjected to western blot analyses for N-cadherin (C), E-cadherin (D), and GAPDH (E). E-cadherin protein levels were reduced to zero by H19 in both cell lines tested (D) and was associated with an up-regulation of mesenchymal marker N-cadherin in H358 cells (C). To test for western blot integrity GAPDH protein level was examined (E).

### *3.5. H19 knockdown attenuates the scattering phenotype induced by HGF/SF in lung carcinoma cells and ablates HGF/SF tumorigenic enhancing property*

We decided to explore the HGF–H19 relationship in lung cancer cell lines. The A549 and H358 cell lines have been reported to express the tyrosine kinase c-Met receptor [31]. When HGF was added at different concentrations to the medium, the luciferase gene product expressed under the transcriptional control of 0.8 kb H19 promoter was up-regulated both in normal and hypoxic cell culture conditions. The H19 promoter was unresponsive to hypoxic stress (Fig. 9A & B). These results are in accordance with a previous study [32].

We present here new evidence showing that the tumorigenic and scattering effect of HGF/SF on the A549 cells can be attenuated by H19 knockdown. HGF/SF treatment resulted in enhancement of *in vitro* tumorigenicity measured by anchorage independent growth through increasing in the number of colonies grown on soft agar in both normoxic and hypoxia recovery conditions (Fig. 9C). In hypoxia recovery conditions cells were first exposed to transient hypoxic stress for 24 h then seeded on soft agar with or without HGF/SF treatment. HGF/SF treatment had a more pronounced effect on increasing colony numbers after hypoxia recovery (Fig. 9C).

The experiment was repeated in cells whose H19 expression had been successfully silenced using H19 siRNA (data not shown). The ability of these H19 knockdown cells to form colonies on soft agar was attenuated (Fig. 9C), consistent with the known oncogenic function of H19 RNA [6]. Moreover, H19 knockdown attenuated the ability of HGF/SF to induce colony formation. The number of colonies formed when cells were transfected with H19 siRNA was significantly less compared to two control groups transfected with siRNA targeting luciferase (si-LUC) and mock transfection (P<0.01). Furthermore, the scattering morphology of the clones induced by HGF/SF was totally dependent on H19 RNA (Fig. 9D). Altogether these results show that in vitro tumoriginicity and the scatering phenotype induced by HGF/SF depend at least in part on H19 RNA. Similar results were obtained in H358 cells using a different H19 siRNA, indicating that the results were specific and not due to an off-target effect of H19 siRNA (data not shown).

## 4. Discussion

During tumor progression, malignant tumors can be reprogrammed into mesenchymal like cells through the process of EMT. This conversion explains how epithelial tumor cells escape their primary sites to form distinct metastasis, the fatal outcome of most cancer types. Recent data even link EMT to cancer stem cells and drug resistance (for review see [24]). So understanding the molecular circuits driving this conversion is vitally important. In the present study, we have provided

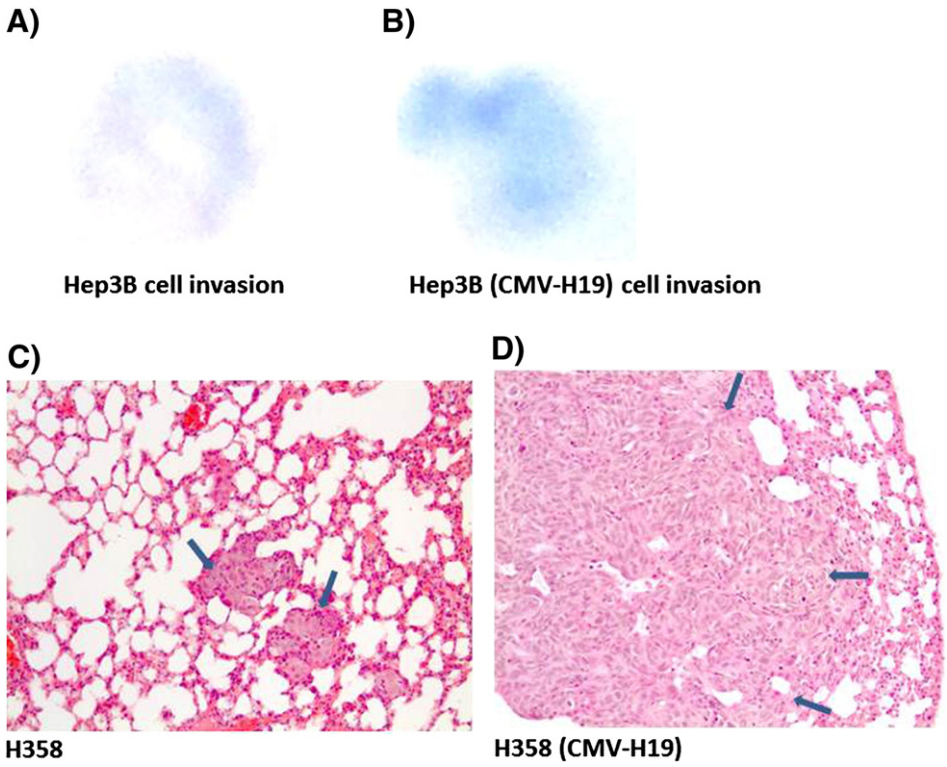


**Fig. 8.** H19 enhanced the invasive potential of Hep3B cells *in vitro* and the metastatic potential of H358 cells *in vivo*. Representative samples for *in vitro* invasion assay for the non-metastatic Hep3B cells (A), compared to the same cell line over-expressing H19 RNA (B). The intensity of the blue dye (Giemsa stain), was directly proportional to the number of cells invading an artificial membrane. Results showed that H19 RNA enhanced the invading potential of Hep3B cells *in vitro*. Representative samples of the lung tissues of mice intravenously injected with H358 lung carcinoma cells (C) and H358 cells over-expressing H19 RNA (D). Results showed small microscopic tumor foci detected after 28 days post injection of H358 parental cells in some of the injected mice lungs. H358 cells over-expressing H19 RNA formed tumors in the majority of the mice lungs, sometimes visible to naked eyes with large microscopic tumor foci. Results showed that H19 RNA enhanced H358 tumor metastasis *in vivo*.

functional and mechanistic evidences of a prominent role played by the H19/miR-675 in promoting metastasis at least in part by being involved in the EMT process.

Although it was discovered nearly thirty years ago [33], key questions regarding H19 gene properties, function and mechanism of action remain to be resolved. Several lines of evidence supporting the involvement of H19 RNA in the metastatic cascade have accumulated over the past few years. Previous reports including those of our own group have identified H19 RNA as one of the genes that is up-regulated by hypoxic stress [6,13], and in response to HGF/SF [32], two of the well established inducers of metastasis. Disease-free survival from the first biopsy to first recurrence was significantly shorter in patients with tumors having a larger fraction of H19 expressing cells [34]. Furthermore we identified H19 downstream targets [6,15] that showed a clear preference towards genes promoting cellular migration, angiogenesis and metastasis. All of these observations and others are in accordance with the idea that the H19 gene may have a role in promoting tumor metastasis, however, the pro-oncogenic events capable of regulating H19 RNA remain largely uncharacterized and furthermore both functional and mechanistic data are absent.

In this study we explored H19's role in the metastatic cascade. As a first step to establishing this role, we showed that H19 is expressed in all metastatic sites examined irrespective of tumor primary origin that may indicate that H19 activation is a general phenomenon of the metastatic event.

Moreover in a mouse mammary cancer cell line model we showed that H19 expression matched metastatic potential. Interestingly, similar results have been obtained by Yang et al. [29, supplementary information], on their study on the importance of Twist as a regulator of EMT. By microarray analyses they have looked at candidate genes regulating this phenotype and found that the most up-regulated gene is H19 RNA, just above Twist itself.

Among the extracellular factors that activate the EMT program, TGF-β, hypoxia, and HGF/SF represent potent EMT inducers. Moreover, the EMT program is linked to multidrug resistance. TGF-β mediates several and sometimes opposite effects on epithelial cells. It can induce both pro- and anti-apoptotic signals in human fetal hepatocytes, and also can induce and maintain EMT [35]. Furthermore evidence provided by numerous studies suggests that hypoxic conditions *"per se"* can trigger, as an independent factor, an EMT program leading different types of human cancer cells to significantly increase invasiveness. HIF-1-regulated genes promote angiogenesis, invasion and EMT, a critical step of metastasis [36].

Interestingly, all EMT master inducers tested in our study induced H19 RNA (also miR-675 when tested) along with EMT markers.

This mechanistically put H19/miR-675 in the core of the EMT process through multiple signaling pathway. One pathway identified in this study is the PI3K–AKT pathway.

A pivotal hallmark of EMT is the loss of E-cadherin expression, which is consistently observed at sites of EMT during development and cancer and which is involved in the transition of adenoma to carcinoma in animal models [37]. Our results show that H19 RNA over-expression abolishes E-cadherin protein, and is sometimes associated with an increase of N-cadherin protein. This effect is miR-675 dependent and associated with Slug but not Snail up-regulation.

These results suggest that H19 may suppress E-cadherin expression by up-regulating Slug, *via* a mechanism that involves miR-675. The exact sequence of events and miR-675 targets require further investigation.

Our results also demonstrate that Slug can up-regulate H19 expression and activate its promoter possibly through an indirect mechanism. Altogether, this may support the existence of a positive feedback loop between H19 and Slug mediated by miR-675 which controls E-cadherin expression. Further investigation is needed to identify

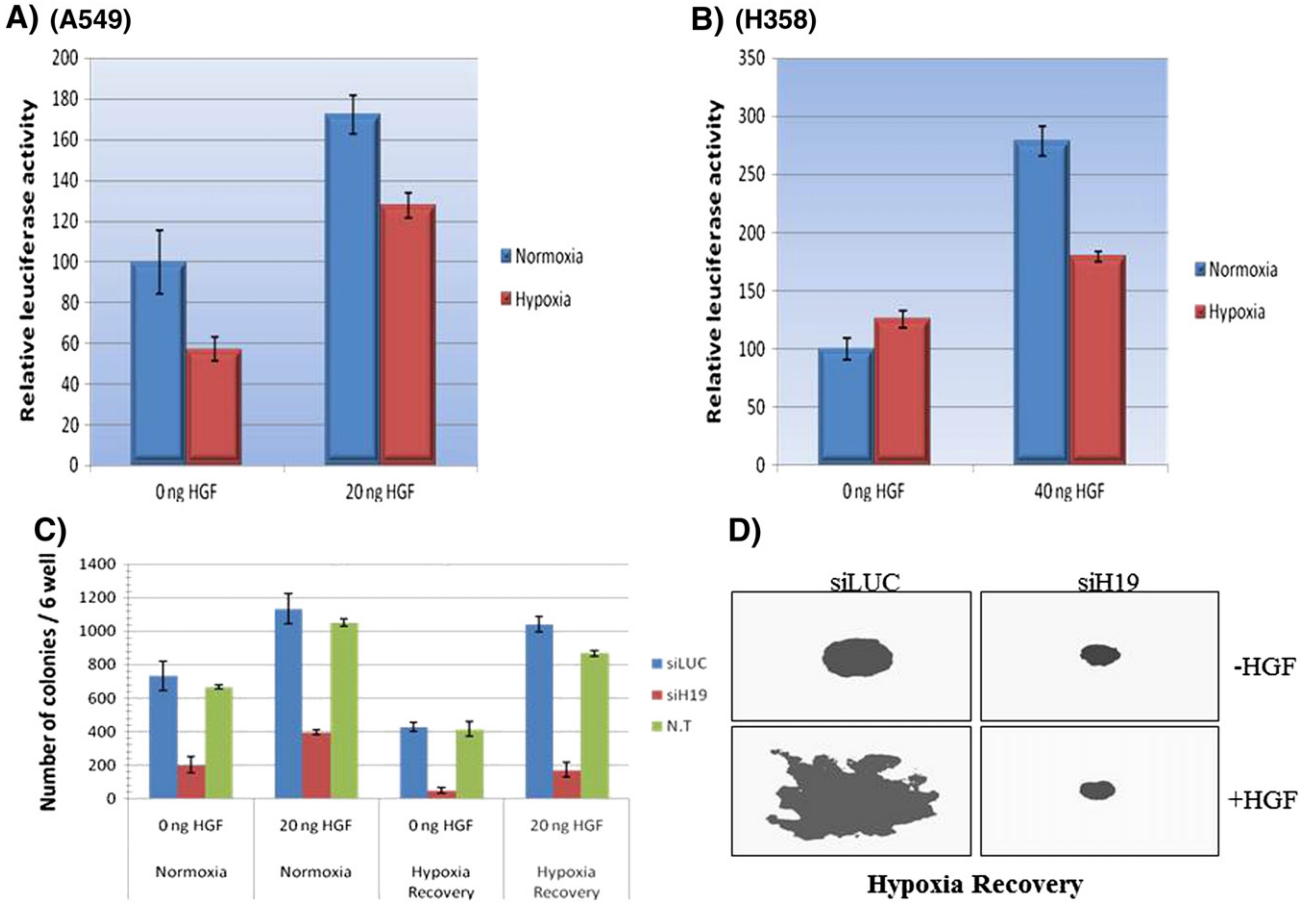


**Fig. 9.** H19 knockdown abolished the scattering effect of HGF/SF, and attenuated colony formation and induction on soft agar. (A & B) A549 and H358 cells (left and right, respectively) were seeded in 12-well plates and transfected with plasmid expressing the luciferase gene under the control of the H19 gene promoter. 24 h post transfection medium was removed and new medium containing 20 or 40 ng/ml of HGF/SF was added to A549 and H358 respecyively. HGF/SF induced H19 promoter activity in both cell lines, in normoxic and hypoxic conditions. (C & D) A549 cells were seeded and next day cells were transfected with 250 pmol of siRNA, in duplicates, targeting the luciferace (siLUC) or the H19 RNA (siH19-1) or left to grow with no treatment (N.T.). 12 h post transfection the medium was renewed and one dish from each duplicate was transferred to hypoxic growth conditions for 24 h while the other dish remained in normal conditions. After 24 h, 5000 cells from each group were seeded in soft agar in six wells dish. Two triplicates of 6-well dishes were seeded (total of six dishes) and for the next 4 weeks cells were left to grow under normal growth conditions. Medium was renewed every 3–4 days and for one of the two triplicate HGF was added in concentration of 20 ng/ml every time upon medium removal. (A) The number of colonies formed in the soft agar for each one of the growth conditions was determined under a light microscope, as described in material & methods. Colonies were dyed using crystal violet 0.05%, counted and photographed under the light microscope.

the miR-675 targets that mediate this process. We hypothesize that this target could be a natural inhibitor of Slug expression, and that this positive feedback loop could be responsible for inducing and then maintaining the mesenchymal phenotype of tumor cells. This hypothesis is presented in Fig. 10.

Our *in vitro* and *in vivo* functional studies indicate that H19 is involved in enhancing invasion and metastasis and also mediates the tumorigenic and scattering phenotypes induced by HGF/SF.

During the writing of this report, two conflicting studies linked H19 to the metastatic cascade [38,39]. H19 enhanced the metastatic potential of bladder cancer cells [38], while suppressed that of the hepatocellular carcinoma, being involved in the mesenchymal to epithelial transition (MET) [39]. However, MET is an integral part of the metastatic cascade that participates in the establishment and stabilization of distant metastases by allowing cancerous cells to regain epithelial properties and integrate into distant organs [40]. H19, thus, could be involved in both EMT and MET.

H19 RNA is one of the most highly expressed genes in embryogenesis and placental development. After birth, it is shut down in most tissues, but reactivated in cancers. It is also reactivated in certain physiological and non-cancerous pathological conditions (for recent review see [8]).

It is well established that numerous physiological processes involving cellular invasion, blastocyst implantation, placental development,

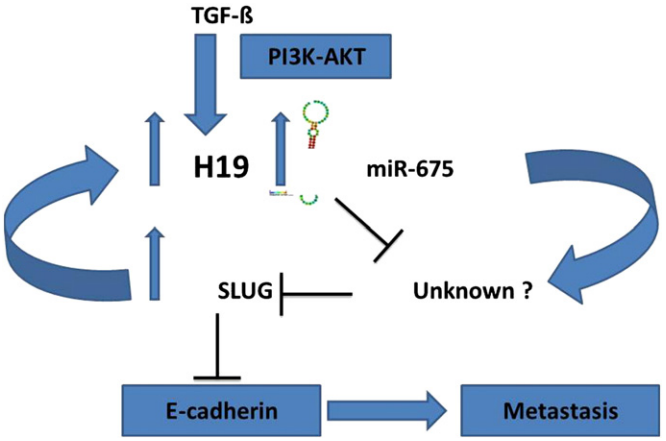


**Fig. 10.** Schematic representation of the hypothesized role of H19/miR675 in the EMT process. Various EMT inducers through multiple signaling pathways (*e.g.* TGF-β through PI3K–AKT pathway) converge to H19/miR675 to up-regulate their levels. These inducers also up-regulate Slug and resulted in suppression of E-cadherin. The mediator of this step is H19/miR675 in a positive feedback loop with Slug through which miR-675 targets an unknown inhibitor for Slug leading to Slug up-regulation, which in turn enhances H19/miR675 levels. This positive feedback loop could account for the induction and maintenance of the mesenchymal phenotype besides explaining the tumorigenic activity of EMT inducers which is largely uncharacterized.

tissue repair and remodeling, wound healing, and loss of pluripotency all involve EMT. Interestingly these physiological processes are manifested by high levels of H19 RNA [41]. Moreover, aberrant EMT also elicits disease development in humans, including rheumatoid arthritis (RA) [42]. It was shown that the PI3K/AKT/HIF-1α pathway is associated with hypoxia-induced EMT in fibroblast-like synoviocytes of RA. Interestingly, RA is nearly the only known non-cancerous pathological process that is associated with activation of H19 RNA [43]. We hypothesize that the mode of H19 gene expression in cancer and in specific physiological and diseased non-cancerous states in adults, has seemingly a common denominator in terms of the triggers and possibly the targets. Activation of H19 by either oncogenic signals or non-cancerous pathological signals activates a common gene program that affects processes common to both events. However, a crucial difference is that in the case of a normal physiological signal, H19 activation is transient, while H19 is persistently activated in cancer.

Although further studies are required to comprehensively define the role of H19 and its micro-RNA in the metastatic cascade, our results not only describe a novel player in the EMT process, but additionally demonstrate the broad range of functions of a lncRNA gene once thought to be no more than a transcriptional noise. We have provided one of relatively few examples in the field of a critical role played by a lncRNA gene in promoting cancer metastasis. While the involvement of EMT inducers in the invasion-metastasis cascade of epithelial tumors is well delineated, their contribution in tumorigenesis remains unclear. On the basis of our previous and current findings, we propose (and confirm it in the case of HGF/SF) that H19 could be one of the central mediators through which those EMT inducers contribute to tumorigenesis.

This further emphasizes the pathological roles played by lncRNA genes and makes them targets in our fight against cancer. Indeed both pre-clinical and clinical studies of BC-819 (a plasmid comprised of the H19 gene regulatory sequences that drive the expression of diphtheria toxin A specifically in tumor cells expressing H19 RNA) show promising outcomes. BC-819-targeted therapy combined with gemcitabine totally ablated metastasis in an aggressive orthotopic pancreatic carcinoma model [44], while clinical trials show promising results in various cancer indications [8]. Our results highlight the importance of targeting H19 RNA, or cells expressing H19 RNA, for therapeutic interventions and the prevention of tumor metastasis, the fatal outcome of all cancer types.

## Financial disclosure

This work was supported by BioCancell Therapeutic (0397706). The funder had no role in study design, data collection and analyses, decision to publish, or preparation of the manuscript.

## Competing interest statement

Professor Abraham Hochberg is also the chief scientist of BioCancell therapeutics.

*Abbreviations*

| | |
|---|---|
| CMV | cytomegalovirus |
| DIG | digoxigenin |
| EMT | epithelial–mesenchymal transition |
| GAPDH | glyceraldehyde 3-phosphate dehydrogenase |
| HGF/SF | hepatocyte growth factor/scatter factor |
| HIF-1α | hypoxia-inducible factors alpha |
| LNA | locked nucleic acid |
| MET | mesenchymal–epithelial transition |
| PBS | phosphate buffered saline |
| PI3K | phosphatidylinositide 3-kinase |
| RT-QPCR | reverse transcriptase quantitative polymerase chain reaction |
| SDS | sodium dodecyl sulfate |
| siRNA | short interfering RNA |
| SSPE | saline sodium phosphate-EDTA |
| SV40 | simian virus 40 |
| TGF-β | transforming growth factor beta |

## Acknowledgements

We give special thanks to Professor Eithan Galun for the critical reading and valuable comments on the manuscript. Rona Harari for providing the plasmid containing the mutated site of miR-675 as part for her PhD thesis. We are also grateful to professor Thomas Wirth for providing EpRAS and XT cells used in this study.

## References

[1] E.W. Thompson, D.F. Newgreen, Carcinoma invasion and metastasis: a role for epithelial–mesenchymal transition? Cancer Res. 65 (2005) 5991–5995.
[2] D. Hanahan, R.A. Weinberg, Hallmarks of cancer: the next generation, Cell 144 (2011) 646–674.
[3] A.D. Rhim, E.T. Mirek, N.M. Aiello, A. Maitra, J.M. Bailey, et al., EMT and dissemination precede pancreatic tumor formation, Cell 148 (2012) 349–361.
[4] M.M. Javle, J.F. Gibbs, K.K. Iwata, Y. Pak, P. Rutledge, et al., Epithelial–mesenchymal transition (EMT) and activated extracellular signal-regulated kinase (p-Erk) in surgically resected pancreatic cancer, Ann. Surg. Oncol. 14 (2007) 3527–3533.
[5] H.J. Maier, T. Wirth, H. Beug, Epithelial–mesenchymal transition in pancreatic carcinoma, Cancers 2 (2010) 2058–2083.
[6] I.J. Matouk, N. DeGroot, S. Mezan, S. Ayesh, R. Abu-lail, et al., The H19 non-coding RNA is essential for human tumor growth, PLoS One 2 (2007) e845.
[7] T. Yoshimizu, A. Miroglio, M.A. Ripoche, A. Gabory, M. Vernucci, et al., The H19 locus acts in vivo as a tumor suppressor, Proc. Natl. Acad. Sci. U. S. A. 105 (2008) 12417–12422.
[8] I. Matouk, E. Raveh, P. Ohana, R.A. Lail, E. Gershtain, et al., The increasing complexity of the oncofetal h19 gene locus: functional dissection and therapeutic intervention, Int. J. Mol. Sci. 14 (2013) 4298–4316.
[9] X. Cai, B.R. Cullen, The imprinted H19 noncoding RNA is a primary microRNA precursor, RNA 13 (2007) 313–316.
[10] P. Onyango, A.P. Feinberg, A nucleolar protein, H19 opposite tumor suppressor (HOTS), is a tumor growth inhibitor encoded by a human imprinted H19 antisense transcript, Proc. Natl. Acad. Sci. U. S. A. 108 (2011) 16759–16764.
[11] N. Berteaux, N. Aptel, G. Cathala, C. Genton, J. Coll, et al., A novel H19 antisense RNA overexpressed in breast cancer contributes to paternal IGF2 expression, Mol. Cell. Biol. 28 (2008) 6731–6745.
[12] I. Matouk, B. Ayesh, T. Schneider, S. Ayesh, P. Ohana, et al., Oncofetal splice-pattern of the human H19 gene, Biochem. Biophys. Res. Commun. 318 (2004) 916–919.
[13] I.J. Matouk, S. Mezan, A. Mizrahi, P. Ohana, R. Abu-Lail, et al., The oncofetal H19 RNA connection: hypoxia, p53 and cancer, Biochim. Biophys. Acta 1803 (2010) 443–451.
[14] D. Barsyte-Lovejoy, S.K. Lau, P.C. Boutros, F. Khosravi, I. Jurisica, et al., The c-Myc oncogene directly induces the H19 noncoding RNA by allele-specific binding to potentiate tumorigenesis, Cancer Res. 66 (2006) 5330–5337.
[15] S. Ayesh, I. Matouk, T. Schneider, P. Ohana, M. Laster, et al., Possible physiological role of H19 RNA, Mol. Carcinog. 35 (2002) 63–74.
[16] N. Berteaux, S. Lottin, D. Monté, S. Pinte, B. Quatannens, et al., *H19* mRNA-like noncoding RNA promotes breast cancer cell proliferation through positive control by E2F1, J. Biol. Chem. 280 (2005) (29625-26636).
[17] T. Dugimont, C. Montpellier, E. Adriaenssens, S. Lottin, L. Dumont, et al., The *H19* TATA-less promoter is efficiently repressed by the wild-type tumor suppressor gene product p53, Oncogene 16 (1998) 2395–2401.
[18] W.P. Tsang, E.K. Ng, S.S. Ng, H. Jin, J. Yu, et al., Oncofetal *H19*-derived miR-675 regulates tumor suppressor RB in human colorectal cancer, Carcinogenesis 31 (2010) 350–358.
[19] M.A. Nieto, The snail superfamily of zinc-finger transcription factors, Nat. Rev. Mol. Cell Biol. 3 (2002) 155–166.
[20] G. Xue, D.F. Restuccia, Q. Lan, D. Hynx, S. Dirnhofer, et al., Akt/PKB-mediated phosphorylation of Twist1 promotes tumor metastasis via mediating cross-talk between PI3K/Akt and TGF-β signaling axes, Cancer Discov. 2 (2012) 248–259.
[21] C.J. Vlahos, W.F. Matter, K.Y. Hui, R.F. Brown, A specific inhibitor of phosphatidylinositol 3-kinase, 2-(4-morpholinyl)-8-phenyl-4H-1-benzopyran-4-one (LY294002), J. Biol. Chem. 269 (1994) 5241–5248.
[22] M. Oft, J. Peli, C. Rudaz, H. Schwarz, H. Beug, et al., TGF-beta1 and Ha-Ras collaborate in modulating the phenotypic plasticity and invasiveness of epithelial tumor cells, Genes Dev. 10 (1996) 2462–2477.
[23] M. Jo, R.D. Lester, V. Montel, B. Eastman, S. Takimoto, et al., Reversibility of epithelial–mesenchymal transition (EMT) induced in breast cancer cells by activation of urokinase receptor-dependent cell signaling, J. Biol. Chem. 284 (2009) 22825–22833.
[24] A. Singh, J. Settleman, EMT, cancer stem cells and drug resistance: an emerging axis of evil in the war on cancer, Oncogene 29 (2010) 4741–4751.
[25] J. Helleman, M. Smid, M.P. Jansen, M.E. van der Berg, E.M. Berns, Pathway analysis of gene lists associated with platinum-based chemotherapy resistance in ovarian cancer: the big picture, Gynecol. Oncol. 117 (2010) 170–176.

[26] A.M. Haslehurst, M. Koti, M. Dharsee, P. Nuin, K. Evans, et al., EMT transcription factors snail and slug directly contribute to cisplatin resistance in ovarian cancer, BMC Cancer 12 (2012) 91.
[27] Y. Fellig, I. Ariel, P. Ohana, P. Schachter, I. Sinelnikov, et al., H19 expression in hepatic metastases from a range of human carcinomas, J. Clin. Pathol. 58 (2005) 1064–1068.
[28] D.L. Dexter, H.M. Kowalski, B.A. Blazar, Z. Fligiel, R. Vogel, et al., Heterogeneity of tumor cells from a single mouse mammary tumor, Cancer Res. 38 (1978) 3174–3181.
[29] J. Yang, S.A. Mani, J.L. Donaher, S. Ramaswamy, R.A. Itzykson, et al., Twist, a master regulator of morphogenesis, plays an essential role in tumor metastasis, Cell 117 (2004) 927–939.
[30] K.M. Hajra, D.Y. Chen, E.R. Fearon, The SLUG zinc-finger protein represses E-cadherin in breast cancer, Cancer Res. 62 (2002) 1613–1618.
[31] A. Hashigasako, M. Machide, T. Nakamura, K. Matsumoto, T. Nakamura, Bi-directional regulation of Ser-985 phosphorylation of c-met via protein kinase C and protein phosphatase 2A involves c-Met activation and cellular responsiveness to hepatocyte growth factor, J. Biol. Chem. 279 (2004) 26445–26452.
[32] E. Adriaenssens, S. Lottin, N. Berteaux, L. Hornez, W. Fauquette, et al., Cross-talk between mesenchyme and epithelium increases H19 gene expression during scattering and morphogenesis of epithelial cells, Exp. Cell Res. 275 (2002) 215–229.
[33] V. Pachnis, A. Belayew, S.M. Tilghman, Locus unlinked to alpha-fetoprotein under the control of the murine raf and Rif genes, Proc. Natl. Acad. Sci. U. S. A. 81 (1984) 5523–5527.
[34] I. Ariel, M. Sughayer, Y. Fellig, G. Pizov, S. Ayesh, et al., The imprinted H19 gene is a marker of early recurrence in human bladder carcinoma, Mol. Pathol. 53 (2000) 320–323.
[35] L. Caja, E. Bertran, J. Campbell, N. Fausto, I. Fabregat, The transforming growth factor-beta (TGF-β) mediates acquisition of a mesenchymal stem cell-like phenotype in human liver cells, J. Cell. Physiol. 226 (2011) 1214–1223.
[36] M.H. Yang, M.Z. Wu, S.H. Chiou, P.M. Chen, S.Y. Chang, et al., Direct regulation of TWIST by HIF-1alpha promotes metastasis, Nat. Cell Biol. 10 (2008) 295–305.
[37] J.P. Thiery, B. Boyer, The junction between cytokines and cell adhesion, Curr. Opin. Cell Biol. 4 (1992) 782–792.
[38] M. Luo, Z. Li, W. Wang, Y. Zeng, Z. Liu, et al., Long non-coding RNA H19 increases bladder cancer metastasis by associating with EZH2 and inhibiting E-cadherin expression, Cancer Lett. 333 (2013) 213–321.
[39] L. Zhang, F. Yang, J.H. Yuan, S.X. Yuan, W.P. Zhou, et al., Epigenetic activation of the MiR-200 family contributes to H19-mediated metastasis suppression in hepatocellular carcinoma, Carcinogenesis 34 (2013) 577–586.
[40] J. Yang, R.A. Weinberg, Epithelial–mesenchymal transition: at the crossroads of development and tumor metastasis, Dev. Cell 14 (2008) 818–826.
[41] I.J. Matouk, P. Ohana, E. Galun, A. Hochberg, The Pivotal Role of the Oncofetal H19 RNA in Human Cancer, A New Hope, Gene Therapy and Cancer Research Focus, Nova Science Publisher, New York, NY, USA, 2008, pp. 241–260.
[42] G.Q. Li, Y. Zhang, D. Liu, Y.Y. Qian, H. Zhang, et al., PI3 kinase/Akt/HIF-1α pathway is associated with hypoxia-induced epithelial–mesenchymal transition in fibroblast-like synoviocytes of rheumatoid arthritis, Mol. Cell. Biochem. 372 (2013) 221–231.
[43] B. Stuhlmüller, E. Kunisch, J. Franz, L. Martinez-Gamboa, M.M. Hernandez, et al., Detection of oncofetal h19 RNA in rheumatoid arthritis synovial tissue, Am. J. Pathol. 163 (2003) 901–911.
[44] V. Sorin, P. Ohana, J. Gallula, T. Birman, I. Matouk, et al., H19-promoter-targeted therapy combined with gemcitabine in the treatment of pancreatic cancer, ISRN Oncol. 2012 (2012) 351750.
[45] R. Kaplan, K. Luettich, A. Heguy, N.R. Hackett, B.G. Harvey, R.G. Crystal, Monoallelic up-regulation of the imprinted H19 gene in airway epithelium of phenotypically normal cigarette smokers, Cancer Res. 63 (2003) 1475–1482.
[46] K.J. Zhang, D.S. Wang, S.Y. Zhang, X.L. Jiao, C.W. Li, et al., The E-cadherin repressor slug and progression of human extrahepatic hilar cholangiocarcinoma, J. Exp. Clin. Cancer Res. 29 (2010) 88.